

# Sequential Waves of Functionally Related Proteins Are Expressed When B Cells Prepare for Antibody Secretion

Eelco van Anken,<sup>1,4</sup> Edwin P. Romijn,<sup>2,4</sup>  
Claudia Maggioni,<sup>1,4</sup> Alexandre Mezghrani,<sup>3</sup>  
Roberto Sitia,<sup>3,5</sup> Ineke Braakman,<sup>1,5,\*</sup>  
and Albert J.R. Heck<sup>2,5</sup>

<sup>1</sup>Department of Bio-organic Chemistry-1  
Bijvoet Center  
Utrecht University  
Padualaan 8  
3584 CH Utrecht

<sup>2</sup>Department of Biomolecular Mass Spectrometry  
Bijvoet Center and  
Utrecht Institute for Pharmaceutical Sciences  
Utrecht University  
Sorbonnelaan 16  
3584 CA Utrecht  
The Netherlands

<sup>3</sup>Università Vita-Salute San Raffaele and  
DiBiT-HSR  
20132 Milano  
Italy

## Summary

Upon encounter with antigen, B lymphocytes differentiate into Ig-secreting plasma cells. This step involves a massive development of secretory organelles, most notably the endoplasmic reticulum. To analyze the relationship between organelle reshaping and Ig secretion, we performed a dynamic proteomics study of B lymphoma cells undergoing *in vitro* terminal differentiation. By clustering proteins according to temporal expression patterns, it appeared that B cells anticipate their secretory role in a multistep process. Metabolic capacity and secretory machinery expand first to accommodate the mass production of IgM that follows.

## Introduction

A key question in cell biology is how cells control the equilibrium of the various organelles to maintain their shape. Even more challenging is how they adjust their architecture to comply with new functions. A spectacular example of such a transformation is the differentiation of B lymphocytes to plasma cells. B lymphocytes express immunoglobulins (Ig) on their surface as clonal antigen receptors but do not secrete antibodies. These cells have a small cytoplasm, with scarce endoplasmic reticulum (ER) cisternae. Upon binding of specific antigen to the B cell receptor or by stimulation with mitogens, B cells proliferate and differentiate into plasma cells, each of which secretes thousands of antibodies per second. In IgM-secreting plasma cells the components of secreted polymers are the secretory form of  $\mu$

heavy chains ( $\mu$ s), light ( $\lambda$ ), and J chains (Reddy and Corley, 1999). This massive Ig production correlates with a highly developed secretory machinery, most being ER (Wiest et al., 1990), like in other professional secretory cells. Many resident ER proteins have been implicated in the folding and assembly of antibody: BiP (Haas and Wabl, 1983) and GRP94 sequentially associate with Ig heavy chains (Melnick et al., 1994), GRP170 was found to bind Ig (Lin et al., 1993), and PDI, ERp72, and many other as yet unidentified microsomal oxidoreductases interact with IgM subunits in a thiol-mediated fashion (Reddy et al., 1996).

We set out to investigate how B lymphocytes reorganize their machineries to become cells that are professional secretors. How does the transformation from dormant B lymphocytes to plasma cells unfold? This question has received little attention. Argon and coworkers followed B cell differentiation by electron microscopy and immunoblotting of some resident ER proteins (Wiest et al., 1990). Two-dimensional electrophoretic analysis of differentiating B cells was performed as early as 1984, but at that time protein identities were not determined (Kettman and Lefkovits, 1984). Recently, Frey et al. made an initial characterization of the proteome of splenocytes, as representatives for B lymphocytes, but limited their analysis to activated cells (Frey et al., 2000).

To follow the differentiation process with time, we chose a dynamic proteomics approach. Using this strategy, we could follow overall changes in protein expression during the reorganization of cellular machineries triggered by the activation of a B lymphocyte. How are Ig secretion and ER development related? At least two possibilities can be envisaged. First, an increase in the synthesis of secretory proteins (Igs) could drive the expansion of the ER via signaling cascades programmed to enhance folding capacity and limit ER load. These regulatory pathways are referred to as the unfolded protein response (UPR) (Patil and Walter, 2001). Alternatively, the development of an efficient protein factory could precede the actual production and release of antibodies.

Here we report that sequential waves of proteins are coordinately expressed during the transformation of B cells into plasma cells. On the first day of activation, mitochondrial and cytosolic chaperones showed highest expression, whereas metabolic enzymes peaked on the third day. ER resident proteins linearly increased during differentiation, accompanied by proteins involved in the redox balance. We witnessed a sharp increase in IgM synthesis only after 2 days of activation. We conclude that the transformation from dormant B cells to secretory plasma cells is a multistep process. Upon activation, B cells carefully prepare for their role as plasma cells well before IgM secretion starts. First, the cell ensures that metabolic capacity and the secretory machinery have expanded enough to accommodate the launch of bulk IgM production.

\*Correspondence: i.braakman@chem.uu.nl

<sup>4</sup>These authors contributed equally to this work.

<sup>5</sup>These authors contributed equally to this work.

## Results

### LPS Induces Ig Secretion and Morphological Changes in I.29 $\mu$ <sup>+</sup> Lymphoma Cells

As a model of B lymphocyte differentiation, we chose the murine B cell lymphoma I.29 $\mu$ <sup>+</sup>, which expresses IgM on the surface but does not secrete antibodies. These cells can be induced by lipopolysaccharide (LPS) to secrete IgM (Stavnezer et al., 1985; Alberini et al., 1987). To confirm their validity as a model of plasma cell differentiation, I.29 $\mu$ <sup>+</sup> cells were treated for 0, 1, 2, 3, or 4 days with LPS. IgM secretion was barely detectable before LPS treatment but increased for 4 consecutive days (Figure 1A, lower panel). In addition to secretion, the total amount of intracellular IgM increased upon activation (Figure 1A, upper panel). Ig secretion correlated with morphological changes that characterize plasma cell differentiation: larger cells displaying an intense intracellular staining by anti-IgM antiserum appeared (Figure 1B), becoming more frequent with time. Concomitantly, the average protein content per cell increased (Figure 1C). Flow cytometry confirmed that most cells increased in size, although not uniformly (Figure 1D). Dividing cells became less frequent as differentiation proceeded (Giemsa and Hoechst 33342 staining, data not shown), and cell death started in the last 2 days of induction (data not shown), which could explain why average protein content started to decrease at day 4.

To further characterize LPS-induced I.29 $\mu$ <sup>+</sup> differentiation, we followed the expression of CD138 (syndecan-1) (Figure 1E, left panel). While only few unstimulated I.29 $\mu$ <sup>+</sup> cells expressed this marker of mature plasma cells (Chilosi et al., 1999), the vast majority of them became positive within day 3 of LPS stimulation. In contrast, expression of CD45 (B220) did not change significantly, possibly because we activated with mitogen instead of antigen (Figure 1E, right panel). The complete set of quantifications of flow cytometry and immunofluorescence experiments is provided on a webpage ([http://vrc.bijvoet-center.nl/boc1/b\\_cells](http://vrc.bijvoet-center.nl/boc1/b_cells)). Taken together, these findings confirm that LPS-induced I.29 $\mu$ <sup>+</sup> cells represent an appropriate model to investigate B cell to plasma cell differentiation in molecular terms (Alberini et al., 1987; Sitia et al., 1985; Stavnezer et al., 1985).

### Drastic Changes of the Proteome upon B Cell Differentiation

To follow changes in protein expression during B cell differentiation, we analyzed postnuclear supernatants from detergent lysates of the I.29 $\mu$ <sup>+</sup> cells before or after activation. To obtain comparable staining intensities, equal amounts of proteins were separated by two-dimensional (2D) gel electrophoresis and visualized either by silver staining or SYPRO Ruby staining. Spot signals were measured by densitometric scanning or fluorescence imaging, respectively. Matching and quantification of spots were performed with the BioRad PDQuest software package. Overall changes in the proteome during B cell differentiation were evident and reproducible, but the pace of the process varied slightly from one experiment to the other. We therefore used a representative experiment for thorough image analysis (Figure 2).

We compared expression kinetics of the ~400 most abundant spots. Because so many protein spots showed strikingly similar expression kinetics, we clustered 75% of detected protein spots in only five distinct synexpression groups. Corresponding to the day of maximal expression, spots were categorized in clusters I (day 0) through V (day 4) (Figure 3A). All other spots were grouped in cluster O. Silver staining and SYPRO Ruby essentially led to the same clustering, despite the broader linear range of SYPRO Ruby. We selected abundant spots from synexpression clusters. Spots were excised and trypsinized. Mass spectrometry revealed the protein identities of 112 spots up to now, representing ~75% of the total signal in the gel.

### Expression Clusters Correlate with Biological Function

Next, we categorized identified proteins by biological function: ER resident proteins, cytoskeletal proteins, cytosolic chaperones, etc. The complete data set of all identified spots is provided on a webpage ([http://vrc.bijvoet-center.nl/boc1/b\\_cells](http://vrc.bijvoet-center.nl/boc1/b_cells)). Most abundant proteins from six functional categories are listed in Figure 4. We found that biological function strongly correlated with synexpression clustering. Where Figure 3A shows their expression clustering, Figure 3B shows, for comparison, the same protein spots clustered by biological function.

A few exceptions aside, we found that the cytoskeleton correlated to cluster I, that cytosolic and mitochondrial chaperones correlated to cluster II, and that metabolic enzymes on average clustered in IV. Three functional groups, ER resident proteins, IgM subunits, and proteins involved in the redox balance, correlated with cluster V. Cluster III contained few proteins, without functional match. Not only did proteins cluster by expression pattern and function, they also clustered by position in the gel, indicating similar mass and pI for proteins of similar function (Figure 3B). Examples of expression kinetics of individual spots are shown in Figure 5A. Apart from the well-established increase of ER proteins and IgM subunits alike (e.g., Wiest et al., 1990), we found, in agreement with previous reports, an upregulation of Cathepsin E (Sealy et al., 1996) and a downregulation of MHC class II  $\beta$  subunit (Silacci et al., 1994; Piskurich et al., 2000). This further validates I.29 $\mu$ <sup>+</sup> cells as an excellent model for B cell differentiation.

By monitoring the changes per biological category we could reconstruct the following series of events in the course of B cell differentiation (Figure 5B). First, mitochondrial and cytosolic chaperones peaked at day 1. Second, metabolic enzymes peaked at day 3. Third, ER resident proteins gradually increased from day 0 to day 4, accompanied by proteins involved in redox balance. Last, after a lag-time of 2 days, the IgM subunits  $\lambda$ ,  $\mu$ , and J chain increased. Whereas  $\lambda$  and  $\mu$  were identified in our proteomics screen (Figure 5A), J chain became detectable only by immunoblotting (Figure 7B). Because data were normalized to total protein amounts per gel, cytoskeletal proteins decreased relative to proteins in other categories (Figures 5A and 5B).

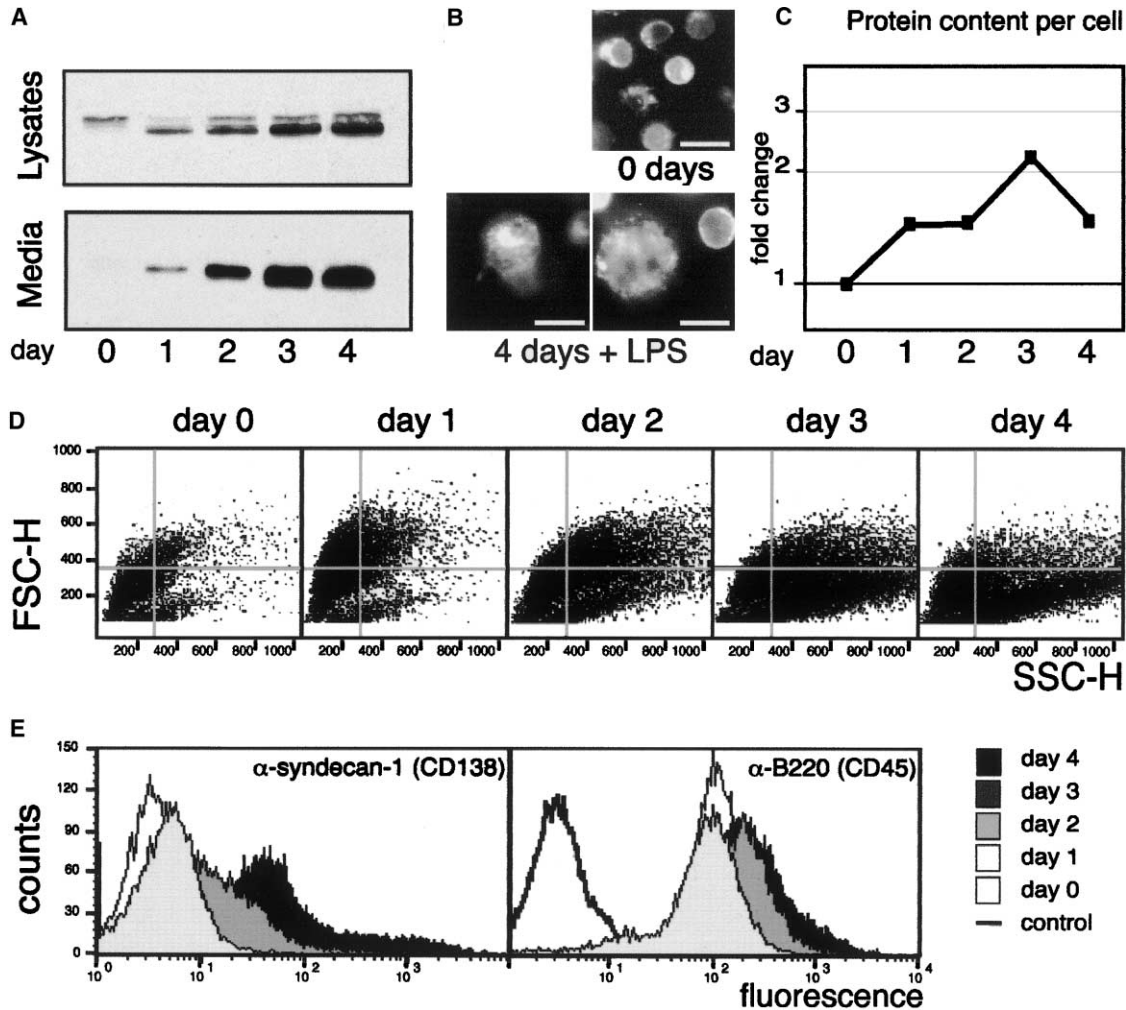


Figure 1. I.29 $\mu^+$  Lymphoma Cells as a Model for B Plasma Cell Differentiation

(A) Induction of IgM secretion. After treatment with LPS for the indicated periods, I.29 $\mu^+$  cells were washed and incubated in fresh medium for 5 hr to follow IgM secretion. Postnuclear lysates (upper panel) and harvested culture media (lower panel) were run on reducing 10% SDS-PAGE gels. Proteins were transferred onto nitrocellulose and decorated with a horse radish peroxidase conjugated anti-IgM antiserum. In the upper panel two bands are visible. Unstimulated I.29 $\mu^+$  cells synthesize approximately equal amounts of  $\mu_m$  and  $\mu_s$  (Sitia et al., 1987). The former are transported to the cell surface, while the latter are degraded intracellularly. The upper band probably corresponds to mature membrane  $\mu$  chains. The lower band contains mixtures of immature, EndoH sensitive membrane and secretory  $\mu$  chains (Fagioli and Sitia, 2001; Sitia et al., 1987).

(B) Appearance of large, IgM-producing cells upon LPS stimulation. LPS-stimulated (day 4, bottom two panels) or untreated I.29 $\mu^+$  cells were grown on coverslips, fixed, permeabilized, and stained with FITC-conjugated anti-IgM antibodies. Bars correspond to 10  $\mu$ m.

(C) Protein concentration of postnuclear lysates was determined. The average of duplicate measurements of two independent experiments was taken for each day to calculate the fold change compared to day 0.

(D) Changes in size and shape in differentiating I.29 $\mu^+$  cells.  $5 \times 10^5$  cells, treated with LPS for the indicated periods, were analyzed by flow cytometry.

(E) Expression of the plasma membrane marker CD138 by LPS-induced I.29 $\mu^+$  cells.  $5 \times 10^5$  cells, treated with LPS for the indicated periods as above, were stained with antibodies specific for CD138 (left panel) or CD45 (right panel) and analyzed by flow cytometry.

### Increase of IgM Synthesis Follows Initial ER Expansion

We found that the increase of IgM subunits follows the initial increase of resident ER proteins. The steady-state levels of intracellular IgM subunits we monitored, however, are the net effect of synthesis, degradation, and secretion. We therefore compared synthesis rates of resident ER proteins and IgM subunits by pulse-labeling cells short enough to render secretion and/or degrada-

tion irrelevant (Sitia et al., 1987). Cells were activated for 0, 1, 2, or 4 days and were radioactively labeled for 10 min after each activation period. Detergent cell lysates were analyzed by 2D gel electrophoresis and normalized for protein content, and signals were detected by phosphor imaging. Signals of proteins and total incorporation of radioactive label were quantified. Labeling abruptly increased the first day, reflecting the overall increase in protein synthesis, only to decrease

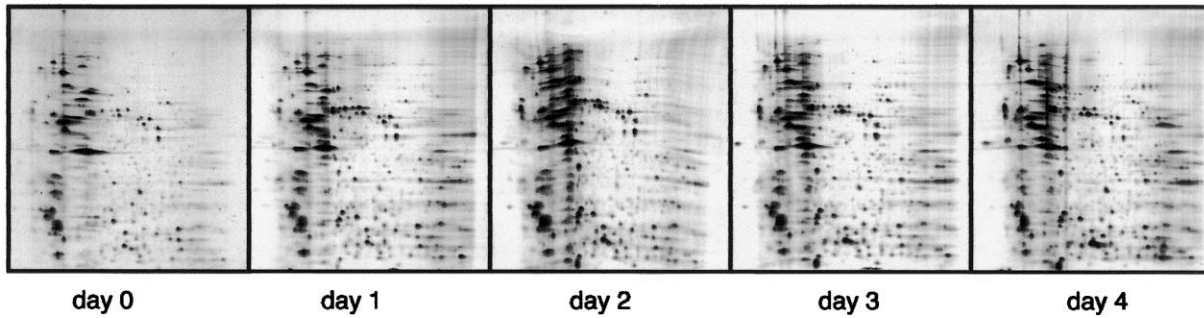


Figure 2. Proteome Changes during I.29 $\mu^+$  Differentiation  
Proteins present in the postnuclear supernatants of I.29 $\mu^+$  cells that were activated with LPS for the indicated times were quantitated as described in the legend to Figure 1C. Similar aliquots were resolved by 2D electrophoresis.

again at day 4 (Figure 6A). Whereas synthesis of resident ER proteins already started to increase on day 1, as shown in Figure 6B for calreticulin, calnexin, and GRP94, synthesis of IgM subunits did not increase until day 2 after activation. We concluded that initial ER expansion indeed preceded bulk IgM biosynthesis and secretion. Continued ER expansion coincided with steeply increased IgM production.

**Initial ER Expansion Does Not Involve a Classical XBP-1-Mediated UPR**

XBP-1 is a prominent UPR signal (Shen et al., 2001; Yoshida et al., 2001; Calfon et al., 2002) but is essential for plasma cell development as well (Reimold et al., 2001). It transduces ER stress to the nucleus as a *trans*-activator of ER resident protein expression (Yoshida et al., 2001). We did not detect XBP-1 on the 2D gels;

hence, to examine the involvement of XBP-1 in ER expansion during differentiation, we analyzed XBP-1 expression by immunoblotting nuclear extracts of differentiating cells. For comparison we analyzed total cell extracts of MEF cells treated with tunicamycin, an agent that provokes a strong UPR. In activated I.29 $\mu^+$  cells (Figure 7A), the 54 kDa form of XBP-1 increased late during differentiation, only reaching high levels after day 2, whereas in tunicamycin-treated cells already after 6 hr a prominent XBP-1 band was detected. Interestingly, most XBP-1 was migrating at a position of  $\sim$ 100 kDa at day 4 of differentiation. This band, also induced in tunicamycin-treated MEF cells, might represent a heterodimer with *c-fos* (Ono et al., 1991). The kinetics of accumulation of XBP-1 matched those of all IgM subunits,  $\lambda$  and  $\mu$  (Figures 5 and 6B) as well as J chain (Figure 7B). We concluded that accumulation of high

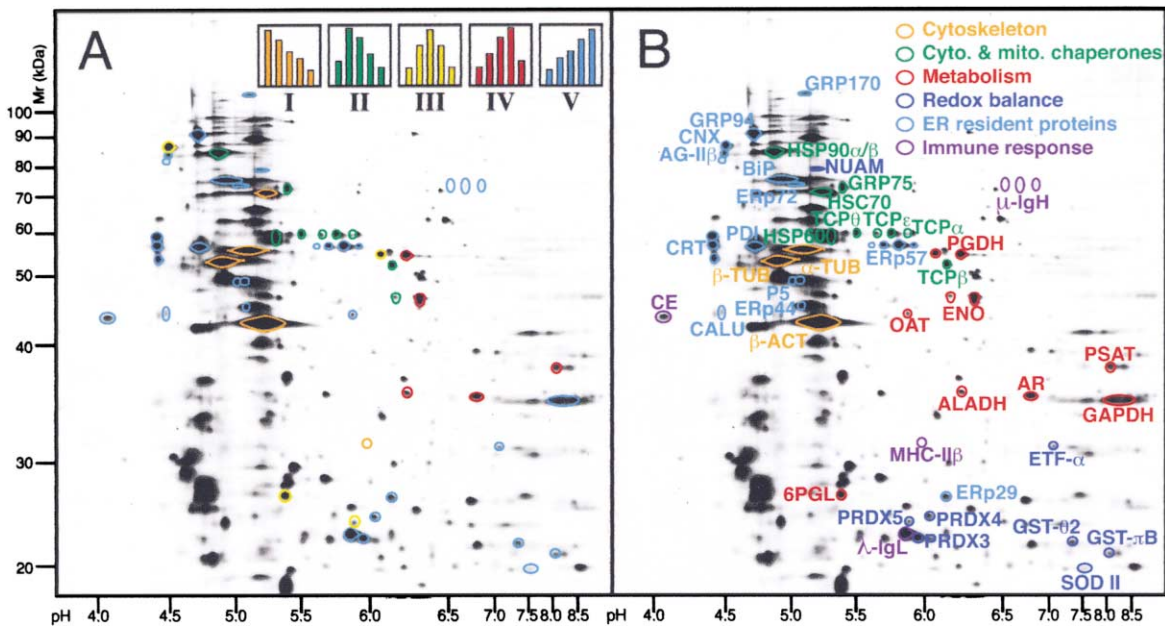


Figure 3. Protein Expression Clusters Correlate to Biological Function  
(A) Spots were clustered based on expression profiles. Spots are color coded per expression cluster. The gel of the third day of activation served as the reference gel.  
(B) Protein identities are indicated, and proteins are color coded per functional category. For abbreviations see Figure 4. The gel of the third day of activation served as the reference gel.

| Functional category      | Cluster | Protein Identity | Swiss Prot Accession No                    | Mr (kDa) |        | pI  |        |     |
|--------------------------|---------|------------------|--|----------|--------|-----|--------|-----|
|                          |         |                  |  | gel      | theory | gel | theory |     |
| Cytoskeleton             | I       | $\beta$ -ACT     | $\beta$ -actin                             | P02570   | 43     | 42  | 5.3    | 5.3 |
|                          | I       | $\alpha$ -TUB    | $\alpha$ -2 tubulin                        | P05213   | 56     | 50  | 5.1    | 5.0 |
|                          | I       | $\beta$ -TUB     | $\beta$ -5 tubulin                         | P05218   | 54     | 50  | 4.9    | 4.8 |
| Cytosolic chaperones     | I       | HSC70            |  | P08109   | 70     | 71  | 5.4    | 5.4 |
|                          | II      | HSP90 $\alpha$   |  | P07901   | 85     | 85  | 5.0    | 5.0 |
|                          | II      | HSP90 $\beta$    |  | P11499   | 85     | 83  | 5.0    | 5.0 |
|                          | II      | TCP $\alpha$     | TCP-1- $\alpha$ subunit                    | P11983   | 60     | 60  | 5.8    | 5.8 |
|                          | II      | TCP $\beta$      | TCP-1- $\beta$ subunit                     | P80314   | 52     | 57  | 6.2    | 6.0 |
|                          | II      | TCP $\epsilon$   | TCP-1- $\epsilon$ subunit                  | P80316   | 60     | 60  | 5.6    | 5.7 |
|                          | II      | TCP $\theta$     | TCP-1- $\theta$ subunit                    | P42932   | 60     | 60  | 5.9    | 5.4 |
| Mitochondrial chaperones | II      | GRP75            |  | P38647   | 72     | 69  | 5.6    | 5.5 |
|                          | II      | HSP60            |  | P19226   | 59     | 58  | 5.5    | 5.4 |
| Metabolism               | IV      | AR               | Aldehyde Reductase                         | P45376   | 36     | 36  | 6.8    | 6.8 |
|                          | IV      | ALADH            | $\delta$ -Aminolevulinic acid dehydratase  | P10518   | 36     | 36  | 6.3    | 6.3 |
|                          | IV      | ENO              | $\alpha$ -Enolase                          | P17182   | 48     | 47  | 6.4    | 6.4 |
|                          | V       | GAPDH            | Glyceraldehyde 3-phosphate DHG             | P16858   | 33     | 36  | 8.3    | 8.5 |
|                          | V       | OAT              | Ornithine AT                               | P29758   | 45     | 46  | 6.0    | 5.5 |
|                          | IV      | PGDH             | Phosphoglycerate DHG                       | Q61753   | 55     | 56  | 6.3    | 6.4 |
|                          | III     | 6PGL             | 6-Phosphogluconolactonase *                | Q9CQ60   | 27     | 27  | 5.4    | 5.6 |
|                          | IV      | PSAT             | Phosphoserine AT                           | Q99K85   | 38     | 41  | 8.1    | 8.2 |
| Redox balance            | V       | ETF- $\alpha$    | Electron transfer flavoprotein- $\alpha$ * | Q99LC5   | 32     | 33  | 7.2    | 7.7 |
|                          | V       | GST- $\theta$ 2  | Glutathione-S transferase $\theta$ 2       | Q61133   | 22     | 28  | 7.3    | 7.2 |
|                          | V       | GST- $\pi$ B     | Glutathione-S transferase $\pi$ B          | P19157   | 21     | 24  | 7.8    | 8.1 |
|                          | V       | NUAM             | NADH-ubiquinone oxidoreductase *           | Q91VD9   | 79     | 77  | 5.2    | 5.2 |
|                          | V       | PRDX3            | Peroxisredoxin-3                           | P20108   | 22     | 22  | 5.7    | 5.9 |
|                          | V       | PRDX4            | Peroxisredoxin-4                           | O08807   | 24     | 31  | 6.1    | 6.7 |
|                          | III     | PRDX5            | Peroxisredoxin-5 *                         | Q91WT2   | 25     | 25  | 5.9    | 7.8 |
|                          | V       | SOD-II           | Superoxide dismutase II                    | P09671   | 20     | 22  | 7.3    | 7.7 |
| ER resident proteins     | V       | AG-II $\beta$    | Alpha-glucosidase II $\beta$ subunit       | O08795   | 85     | 59  | 4.5    | 4.4 |
|                          | V       | BiP              |  | P20029   | 74     | 70  | 5.1    | 5.0 |
|                          | III     | CNX              | Calnexin                                   | P35564   | 90     | 65  | 4.5    | 4.5 |
|                          | V       | CRT              | Calreticulin                               | P14211   | 58     | 46  | 4.3    | 4.3 |
|                          | V       | CALU             | Calumenin                                  | O35887   | 45     | 35  | 4.5    | 4.5 |
|                          | V       | ERp29            |  | P57759   | 25     | 26  | 6.2    | 5.7 |
|                          | V       | ERp44            | *  | Q9D1Q6   | 44     | 44  | 5.1    | 5.1 |
|                          | V       | ERp57            |  | P27773   | 58     | 54  | 5.9    | 5.8 |
|                          | V       | ERp72            |  | P08003   | 73     | 70  | 5.2    | 5.0 |
|                          | V       | GRP94            |  | P08113   | 93     | 90  | 4.7    | 4.7 |
|                          | V       | GRP170           |  | Q9JKR6   | 120    | 107 | 5.2    | 5.1 |
|                          | V       | PDI              |  | P09103   | 58     | 55  | 4.7    | 4.8 |
|                          | V       | P5               | *  | Q922R8   | 49     | 46  | 5.1    | 5.0 |
| Immune response          | V       | CE               | Cathepsin E                                | P70269   | 43     | 43  | 4.1    | 4.5 |
|                          | V       | $\lambda$ -IgL   | $\lambda$ Ig Light chain                   |          | 23     |     | 5.9    |     |
|                          | V       | $\mu$ -IgH       | $\mu$ Ig Heavy chain                       |          | 73     |     | 6.9    |     |
|                          | I       | MHC-II $\beta$   | MHC class II $\beta$ subunit               |          | 32     |     | 5.9    |     |

Figure 4. Protein Identity List

Proteins are listed per functional category. Cluster numbers are indicated for comparison. SwissProt accession numbers, theoretical and apparent molecular weights, and pI are indicated, except for IgM and MHC II subunits (because of idiotypic variation). Proteins that were identified by similarity to homologs in other species are marked (\*).

levels of XBP-1 did not precede the increased load of IgM in the ER, suggesting that while the first stage of ER expansion did not involve a classical UPR, the ER load that starts at day 3 does activate a classical, cargo-induced XBP-1-mediated UPR.

## Discussion

Following B cell differentiation by a dynamic proteomics approach gave us a broad, unbiased view of the changes that occur. We found that the vast majority of spots varied substantially with time, whereas, for instance, in the bacterial cell cycle only 15% of spots change (Grunenfelder et al., 2001). Upon analysis of the changes of highly abundant proteins, representing six important cellular machineries, we concluded that the B cell carefully prepares for its secretory role.

### Functionally Related Clusters of Proteins Appear in Waves

Because expression clusters correlated to functional groups, a picture emerged of the series of events that

occur in the course of B cell differentiation. Mitochondrial and cytosolic chaperones were upregulated early. Metabolic enzymes peaked later. ER resident folding factors and redox balance proteins were linearly upregulated until the end. In contrast, IgM subunits increased exponentially, after a lag time of 2 days. We normalized our analyses based on the amount of protein in the gel, resulting in a relative decrease of cytoskeletal proteins. From the increase in protein content of cells, however, we calculated that cytoskeletal proteins in fact slightly increased per cell. As a consequence, the increases we observed for other clusters are more dramatic than shown (e.g., after 4 days of activation, ER proteins have increased 15-fold compared to cytoskeleton). Per differentiating cell, even this factor of 15-fold is likely an underestimate since at day 4 not all cells had fully differentiated yet.

Although we found a few exceptions, the correlation between expression timing and protein function was evident. For instance, 11 out of the 12 known ER proteins (ERps) we identified belonged to expression cluster V. By reversing this argument, can the temporal expression

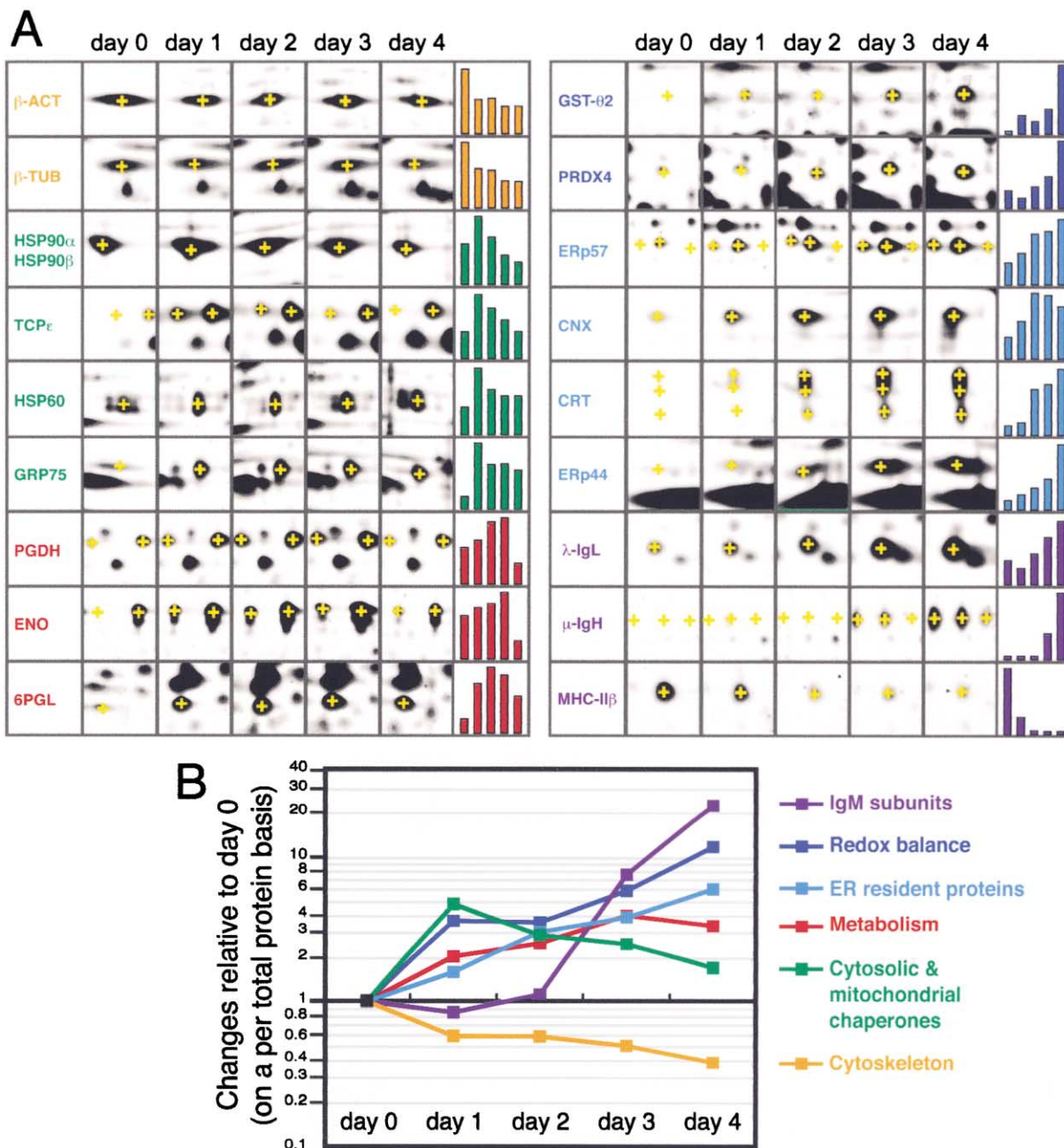


Figure 5. Changes in Expression Levels per Functional Category Reveal a Series of Events during Differentiation

(A) Excerpts from 2D gels of each day from a representative B cell activation experiment are shown for a few proteins per functional group. Proteins of interest are marked (+). Their expression kinetics, determined by densitometry, are depicted in histograms on the right. Spot quantity of the day of maximal expression was set at 100%. For proteins that were present in more than one spot, all of these spots are marked, and histograms represent the sum of these spots.

(B) For all identified proteins, represented in Figure 4, spot quantities at every day of activation were divided by the spot quantity before activation (day 0), to calculate the fold change of proteins during the course of differentiation. If a protein was represented by more than one spot, the sum of spot quantities was used. The changes of all proteins listed in Figure 4 were averaged per functional category. Day 0 was set at 1 and changes in expression level per functional category were plotted logarithmically, to give a similar deviation from the x axis for a y-fold increase as for a y-fold decrease.

pattern of a protein be exploited to predict its functional role? Indeed, we identified several novel proteins that followed the cluster-function relationship. For example, we found a protein in cluster V, that carried hallmarks of ER resident proteins, being an N-terminal signal sequence needed for targeting to the ER, a C-terminal

tetrapeptide RDEL that mediates ER residency, and a putative CRFS redox active site. We named this protein ERp44. Evidence that ERp44 is indeed a bona fide ER folding assistant has been obtained in the meantime (Anelli et al., 2002).

Remarkably, protein categories also clustered in the

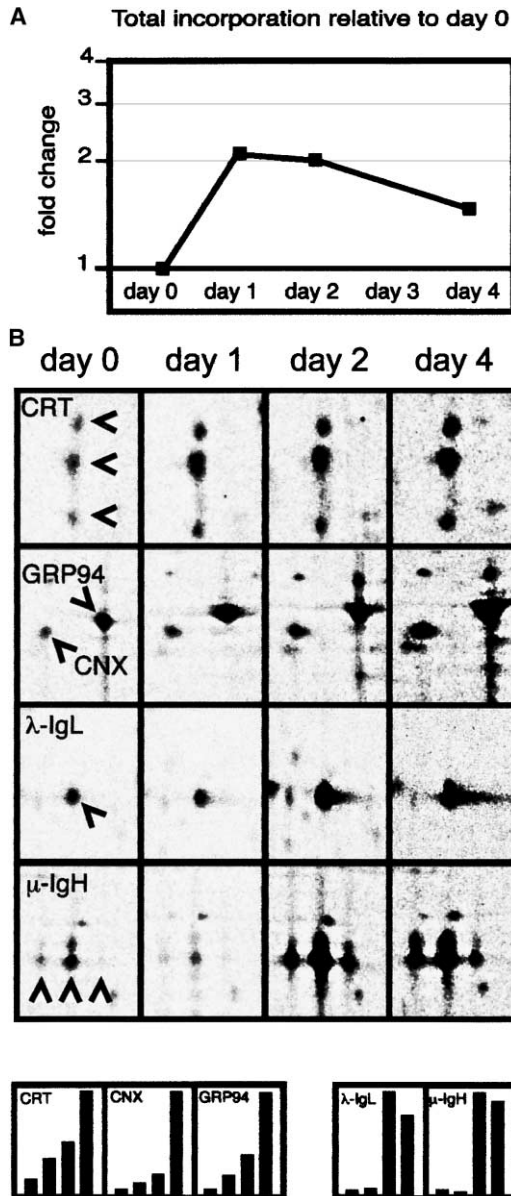


Figure 6. Expansion of the ER Precedes the Increase in IgM Synthesis

(A) After exposure to LPS for the indicated times, cells were pulse labeled with radioactive amino acids for 10 min. Postnuclear supernatants of cell lysates were resolved by one-dimensional SDS-PAGE, and newly synthesized proteins were quantified by phosphor imaging. Changes in incorporation per day were calculated as described for Figure 5B.

(B) Aliquots of the same samples were analyzed by 2D electrophoresis. Radioactive signals were detected by phosphor imaging and identified as in Figures 3 and 5. Excerpts of gels show synthesis levels of three ER proteins, calnexin (CNX), GRP94, and calreticulin (CRT), and two IgM subunits, light chain ( $\lambda$ -IgL) and heavy chain ( $\mu$ -IgH), at different time points after activation. Proteins of interest are marked (>). Signals were quantified and depicted in histograms (bottom panels). For each spot, the most intense signal (comparing days) was set at 100%.

gel. The tendency of resident ER proteins to focus at acidic pH may be a consequence of their  $\text{Ca}^{2+}$  binding properties (Glu/Asp stretches) (Lucero et al., 1998). Many cytosolic proteins, whose folding may be facili-

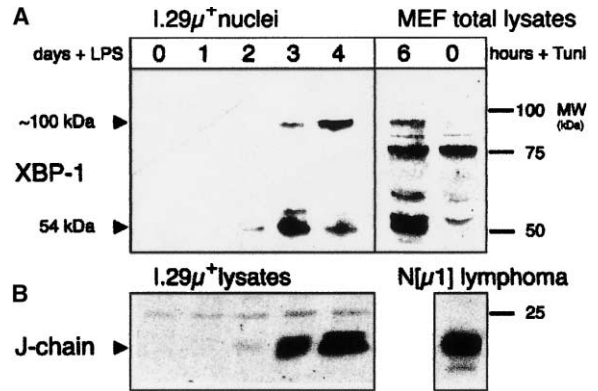


Figure 7. ER Expansion in Differentiating I.29 $\mu^+$  Precedes Activation of XBP-1

(A) Nuclei were isolated from differentiating I.29 $\mu^+$  cells and resuspended in sample buffer. DNA was destroyed by shearing and sonication. The equivalent of  $5 \times 10^5$  nuclei was loaded per lane. Lysates of MEF cells treated with or without 10  $\mu\text{g/ml}$  tunicamycin for 6 hr were also analyzed by SDS-PAGE under reducing conditions. Nitrocellulose blots were decorated with rabbit anti-XBP-1 antibodies followed by horseradish peroxidase conjugated goat anti-rabbit and revealed by ECL.

(B) Postnuclear lysates from differentiating I.29 $\mu^+$  cells were subjected to SDS-PAGE and transferred to nitrocellulose as in (A), followed by decoration with antibodies against J chain. Lysates from a murine myeloma (N[ $\mu$ 1] [Sitia et al., 1987]), were analyzed as a positive reference.

tated by entering into chaperonin cages, tend to be smaller than 70 kDa. For other clusters the colocalization on gels is less easily understood. Possibly, protein function or the specific milieu within compartments defines what pI and MW range are optimal. This would explain why, despite low sequence identity, the pI of many proteins has been conserved from yeast to mammals (E.v.A., unpublished data).

#### Getting Prepared: Providing Energy and Supplies

The synthetic requirements of this dramatic cellular expansion likely explain the instantaneous increase of most mitochondrial and cytosolic chaperones, except, not surprisingly, the nonstress-inducible HSC70 (Ingolia and Craig, 1982). Their instantaneous upregulation apparently is essential to sustain energy and protein production. As discussed above, the subsequent decrease in this class of proteins is again relative. The cells seem to anticipate their future needs for these proteins, since they are upregulated rapidly to a level that is sufficient throughout the entire differentiation process.

On average, metabolic enzymes peaked at 3 days after activation. The upregulation of the glycolytic enzymes glyceraldehyde 3-phosphate dehydrogenase and  $\alpha$ -enolase likely reflects the increase in energy requirements. Increased levels of ornithine aminotransferase, phosphoglycerate dehydrogenase, and phosphoserine aminotransferase may be necessary to facilitate the metabolism of amino acids, serine in particular, to sustain the rise in protein synthesis. The emphasis on serine synthesis could reflect the need of this amino acid for both protein and lipid synthesis; phosphatidylserine may be needed for membrane expansion. The transient upregulation of 6-phosphogluconolactase may reflect

membrane expansion and/or a change in redox balance. This enzyme is involved in the pentosephosphate pathway, which generates NADPH, a redox-active molecule a.o. necessary for fatty acid synthesis. The upregulation of  $\delta$ -aminolevulinic acid dehydratase, involved in heme synthesis, may reflect the growing need of heme for cytochrome synthesis. Total metabolic activity, as monitored by incorporation of radioactive label, rapidly increased 2-fold the first day of activation only to decrease at day 4. Altogether, these data indicate that the cell first needs energy, as well as protein and membrane synthesis for expansion. Later, metabolic activity can be lower again since now the cell is fully expanded and “only” needs energy for IgM production and maintenance of the new equilibrium.

### Redox Balance during Differentiation

As opposed to the cytosol, the ER maintains an oxidative environment (Hwang et al., 1992). Since the ER expands immensely, the cell on average may become more oxidative. Most proteins involved in the redox balance, residing outside of the ER in the cytosol and mitochondria, were linearly upregulated in the same fashion as resident ER proteins. Redox proteins could buffer against oxidative stress leaking out of the ER (Tu and Weissman, 2002). Alternatively, these redox proteins may function to help provide and maintain or influence the oxidative environment in the ER, perhaps to support IgM polymerization. Although in B lymphocytes secretory  $\mu$  chains are synthesized and assembled into  $\mu_2\lambda_2$  “monomers,” these do not assemble into polymers (Shahar et al., 1992). Upon B cell activation, IgM monomers start to polymerize via interchain disulfide bonds, concomitant with the beginning of detectable J chain expression. Expression of J chains in activated B cells is not required for polymerization per se, but rather ensures that pentamers are formed (Brewer et al., 1994). The sudden change in the tendency of IgM monomers to form interchain disulfide-linked polymers may be facilitated by a switch in the redox balance in the ER (Sitia et al., 1990). Redox active proteins could be indirectly involved in either the prevention of polymerization in B cells or in the stimulation of polymerization in a plasma cell.

### Collective Increase of ER Proteins

We witnessed a continuous increase of ER resident proteins throughout the differentiation process, such that at four days after activation a quarter of the total signal in the gel represented ER proteins. The upregulation of resident ER proteins was coordinated such that their relative abundance was almost constant. A notable exception was the relative decrease of calnexin (CNX) within the ER at steady-state levels, despite its increased de novo synthesis. Interestingly, this coincided with an increase of the calreticulin (CRT) pool. Perhaps CRT can compensate for the relative decrease of CNX, since CNX and CRT are functionally related proteins (Trombetta and Helenius, 1998). For the remainder, we found no indications that any known ER proteins be recruited specifically during differentiation, although this has been reported for ERp72 and GRP94 (Wiest et al., 1990). Either all identified ER proteins are required

for the maturation of IgM or the ER can only expand en bloc. This would be consistent with the fact that ER proteins share *cis*-acting elements in their promoter region: ER stress elements (ERSE) (Yoshida et al., 1998; Roy and Lee, 1999; Kokame et al., 2001) or unfolded protein response elements (UPRE) (Wang et al., 2000; Yoshida et al., 2001).

### Does IgM Drive ER Expansion?

An important regulatory machinery for ER expansion is represented by the unfolded protein response (UPR). Although the UPR is much more complex in mammals than in yeast, one pathway has been conserved: the Ire1 pathway (reviewed in Patil and Walter, 2001; Lee, 2001; Ma and Hendershot, 2001). The Ire1 proteins have an unfolded protein sensor domain in the ER lumen. Upon accumulation of unfolded proteins, the effector domain of Ire1 in the cytosol splices the mRNA of the transcription factor Hac1p in yeast (Patil and Walter, 2001) or its mammalian homolog XBP-1 (Shen et al., 2001; Yoshida et al., 2001; Calfon et al., 2002). After religation of their transcript, Hac1p and XBP-1 are synthesized and enhance expression of resident ER proteins through *trans*-activation of the ERSEs (for XBP-1) (Yoshida et al., 2001) or UPREs (for both XBP-1 and Hac1p) (Patil and Walter, 2001; Yoshida et al., 2001) in their promoter regions. Increased levels of resident ER proteins, in turn, are supposed to reinforce the folding and assembly capacity of the ER. Indicative of the importance of the UPR in full B cell differentiation is that mice lacking XBP-1 have normal B cells but no Ig-secreting plasma cells (Reimold et al., 2001).

We show that during B cell differentiation IgM production follows rather than precedes the initial ER expansion; hence, IgM is unlikely to be its driving force. This indicates that the first stage of ER expansion bypasses the classical UPR mechanism, apparently via signals initiated by mitogen or antigen stimulation, such as Blimp-1, a key regulator of B cell differentiation (Shaffer et al., 2002; Turner et al., 1994). The sudden increase in synthesis of IgM subunits after 2 days and the subsequent accumulation of intracellular IgM subunits, however, does seem to trigger a classical XBP-1 ER load-dependent UPR. Only then, after 3 days of activation, did XBP-1 reach high levels, as had been reported earlier for primary splenic B cells (Calfon et al., 2002).

Interestingly, mouse embryonic fibroblasts lacking Ire1 have an intact UPR (Lee et al., 2002). Rather than for the UPR per se, the Ire1/XBP-1 pathway seems necessary for the development of secretory cells: XBP-1 is crucial for liver development (Reimold et al., 2000) and Ire1 for gut development in *C. elegans* (Shen et al., 2001). This suggests that the two-stage launch of ER expansion we observed in B cells may be common to and essential for all cells that differentiate into professional secretors. They first prepare themselves meticulously so as to embark on their new career. Once the first steps are taken, the increased production of cargo may provide a UPR-linked feed-forward circuit that drives further ER expansion (Reimold et al., 2001) and ultimately leads to cell death.

## Experimental Procedures

### Cell Culture and Activation of B Cells

We used the I.29 $\mu$ <sup>+</sup> (IgM,  $\lambda$ ) lymphoma cell line as model B lymphocytes (Alberini et al., 1987). Cells were cultured in suspension in RPMI (Life Technologies) supplemented with 10% fetal calf serum LPS free (FCS, Hyclone), glutamax (1 mM), penicillin (100 U/ml), and streptomycin (100  $\mu$ g/ml), sodium pyruvate (1 mM) and  $\beta$ -mercaptoethanol (50  $\mu$ M). For differentiation experiments cells were incubated in the presence of 20  $\mu$ g/ml LPS (Sigma). Cells were harvested before and after 1, 2, 3, or 4 days of differentiation.

### Western Blotting

Cells were washed in phosphate-buffered saline (PBS, Life Technologies). Fresh culture medium containing 2% FCS was added. Cells were incubated for 5 hr in the presence of LPS before cells were pelleted. Culture media were collected, and cells were lysed in MNT (20 mM MES, 100 mM NaCl, 30 mM Tris-HCl [pH 7.4]), containing 1% Triton X-100 and protease inhibitors (chymostatin, leupeptin, aprotinin, pepstatin A, and PMSF). Cell lysates were centrifuged for 10 min at 17,000 $\times$  g to pellet nuclei. Proteins from postnuclear supernatants from lysates or from culture media were analyzed using 10% sodium dodecyl sulfate polyacrylamide (SDS-PA) gels, and proteins were transferred onto nitrocellulose. The nitrocellulose was saturated with 3% fat free milk (Protifar, Nutricia) for 1 hr, and then incubated with horseradish peroxidase-conjugated anti-IgM or anti-J chain antibodies for 1 hr. For XBP-1 detection, nuclear pellets from lysates of equal numbers of cells per time point were solubilized in sample buffer (200 mM Tris [pH 6.8], 3% SDS, 10% glycerol, 1 mM EDTA, and 0.004% bromophenol blue), forced through a needle, sonicated, and heated for 5 min at 95°C. SDS-PAGE and protein transfer onto nitrocellulose was performed as described above. The nitrocellulose was incubated with a polyclonal rabbit anti XBP-1 antibody (Santa Cruz). Antibody binding was detected via ECL (Amersham) and Biomax MR (Kodak) film.

### Immunofluorescence

Cells were adhered onto poly-L-lysine (Sigma) coated multipot slides for 30 min at 37°C. Cells were fixed in 3% paraformaldehyde for 15 min and permeabilized with 0.1% NP-40 for 10 min. Next, cells were incubated with an FITC-conjugated anti-IgM antibody. IgM expression was monitored by fluorescence microscopy.

### FACS Analysis

R-PE anti-mouse CD138, biotinylated anti-mouse CD45/B220 and FITC-Streptavidin were from BD Pharmingen (San Diego, CA). At least  $5 \times 10^5$  I.29 $\mu$ <sup>+</sup> cells activated for various periods of time were washed in PBS and incubated for 30 min with 200  $\mu$ l of 2.4G2 hybridoma supernatant and 10% rat serum to block Fc receptors (kind gifts of A. Mondino, DiBiT-HSR, Milan). Cells then were stained with relevant antibodies for 30 min at 4°C in the dark. Flow cytometry data were obtained with a FACSCalibur (BD Biosciences) and analyzed using the CellQuest software (BD Biosciences).

### Two-Dimensional Gel Electrophoresis

Cells were washed twice in ice-cold 0.25% sucrose (w/v), 25 mM HEPES-KOH (pH 7.0), and lysed in a small volume of the same solution, containing 1% Triton X-100 and protease inhibitors cocktail. Cell lysates were centrifuged for 10 min at 17,000 $\times$  g to pellet nuclei. Protein concentrations of postnuclear supernatants were determined by DC Protein Assay kit (Biorad). Approximately 200  $\mu$ g of proteins from postnuclear lysates were dissolved in reswelling solution (6.0 M urea [Boehringer], 1.9 M thiourea [Sigma], 4% Triton X-100 [Sigma], 15 mM DTT, and 0.5% [v/v] carrier ampholytes pH 3–10 [AP Biotech]). After reswelling of 18 cm Immobiline DryStrips (pH 3–10) nonlinearized (AP Biotech) with our samples, proteins were separated in the first dimension and on subsequently on 10% SDS-PA gels in the second dimension. This technique allows analysis of many proteins but is not exhaustive (Gygi et al., 2000).

### Image Analysis and Data Processing

Protein spots were visualized by silver staining or by SYPRO Ruby staining (Molecular Probes). Signals from proteins were detected

by densitometric scanning of silver stained gels or by fluorescence imaging of SYPRO Ruby stained gels. Spot detection and matching of spots between gels was performed with the PDQuest software package, version 6.0 (Biorad). The 2D gel of the third day of differentiation was the basis for an in silico "reference gel." Normalization between gels was based on total protein amount (i.e., the total signal of valid spots) per gel. Spot intensities were expressed in parts per million (ppm) of total spot intensity per gel. Background was set at 80 ppm and if the intensity of a spot was below 80 ppm at any time point, we corrected this to background, i.e., 80 ppm. If a spot had a lower intensity than 200 ppm (2.5 $\times$  background) in every gel, the spot was removed from the analysis set. The remaining 409 spots were clustered according to expression kinetics as follows. If spot intensities differed more than 2-fold between at least two points, we determined at which time point expression was maximal. To determine whether only a single maximum in expression existed, we set the following criteria. The spot intensity of the time point adjacent to the maximum should not be more than 2-fold lower than the spot intensity at one time point further from the maximum, etc. If spots had a single maximum according to the above criteria, they were categorized into clusters I, II, III, IV, or V, corresponding to highest expression levels at day 0, 1, 2, 3, or 4. All other spots were grouped in cluster 0. Calculations and formulas can be found as supplemental material ([http://vrc.bijvoet-center.nl/boc1/b\\_cells](http://vrc.bijvoet-center.nl/boc1/b_cells)).

### Mass Spectrometric Analysis of Protein Spots

Spots were excised and digested with trypsin (Roche Diagnostics, GmbH, sequencing grade), and peptide mixtures from in-gel digests were purified and concentrated. Peptides were subjected to mass spectrometric analysis as described previously (Wilm et al., 1996) with some modifications (our unpublished data). Peptide mass fingerprints were acquired on a Voyager DE-STR (Perceptive Biosystems) reflectron time of flight (TOF) mass spectrometer. Peptide sequences were determined by nanoES tandem MS on a quadrupole time of flight mass spectrometer (Q-TOF, Micromass, Manchester, UK) or by MALDI tandem MS on a MALDI quadrupole time of flight mass spectrometer (MALDI-Q-TOF, Micromass, Manchester, UK), or by UltraFlex-TOF/TOF (Bruker Daltonics, Bremen, Germany).

### Protein Identification

Protein identities were revealed either by comparison of peptide mass fingerprints to the theoretical peptide masses of all available proteins in the database, using Profound (Zhang and Chait, 2000), or by comparison of sequence tags from tandem MS analyses to the sequences of proteins or translated ESTs in all public databases, using the peptide sequence tag tool (Mann and Wilm, 1994) and the MS BLAST tool (Shevchenko et al., 2001).

### Metabolic Labeling

Cells were washed once in Hanks' balanced salt solution (Life Technologies) and preincubated in starvation medium lacking methionine and cysteine for 15 min at 37°C. Cells were pulse labeled for 10 min with 50  $\mu$ Ci of Redivue pro-mix L-[<sup>35</sup>S] in vitro labeling mix (AP Biotech). Next, cells were detergent lysed, and postnuclear lysates were analyzed on 2D gels as described above. In addition, lysates were analyzed on reducing 1D 10% SDS-PAGE. Gels were dried between Cellophane (Biorad) sheets before exposure of storage phosphor screens (Kodak). Signals of radioactively labeled proteins were detected with the BioRad Personal Molecular Imager and quantified using the Biorad QuantityOne software package. Total incorporation of label was quantified from the 1D.

### Acknowledgments

We thank JaapWillem Back, Luitzen de Jong, and Anton Muijers for sharing their proteomics expertise, which gave the project a flying start, Alfred Meijer for his expert advice on the interpretation of metabolic phenomena, Mirjam Damen and Elena Ruffato for their invaluable contributions to the various experiments, Danny Schildknecht and Claudio Fagioli for their technical support, Anja Hauser (DRFZ, Berlin) and Anna Mondino (DiBiT, Milan) for reagents and helpful advice for flow cytometry, and Bas Leeftang for advice on creating the website. We are grateful to Gert Folkerts and members

of the Braakman, Sitia, and Heck labs for fruitful discussions. This work was in part supported through grants from NWO-MW (E.v.A. and I.B.), from NWO-CW (A.J.R.H.), from AIRC and the Italian Ministry of Research Center of Excellence in Physiopathology of Cell Differentiation (R.S.), Telethon (C.M. and R.S.), and the EU (Marie Curie Research Training Grant; C.M. and A.M.).

Received: June 7, 2002  
Revised: December 19, 2002

## References

- Alberini, C., Biassoni, R., DeAmbrosio, S., Vismara, D., and Sitia, R. (1987). Differentiation in the murine B cell lymphoma I.29: individual  $\mu$  + clones may be induced by lipopolysaccharide to both IgM secretion and isotype switching. *Eur. J. Immunol.* **17**, 555–562.
- Anelli, T., Alessio, M., Mezghrani, A., Simmen, T., Talamo, F., Bachi, A., and Sitia, R. (2002). ERp44, a novel endoplasmic reticulum folding assistant of the thioredoxin family. *EMBO J.* **21**, 835–844.
- Brewer, J.W., Randall, T.D., Parkhouse, R.M., and Corley, R.B. (1994). IgM hexamers? *Immunol. Today* **15**, 165–168.
- Calfon, M., Zeng, H., Urano, F., Till, J.H., Hubbard, S.R., Harding, H.P., Clark, S.G., and Ron, D. (2002). IRE1 couples endoplasmic reticulum load to secretory capacity by processing the XBP-1 mRNA. *Nature* **415**, 92–96.
- Chilosi, M., Adami, F., Lestani, M., Montagna, L., Cimarosto, L., Semenzato, G., Pizzolo, G., and Menestrina, F. (1999). CD138/syndecan-1: a useful immunohistochemical marker of normal and neoplastic plasma cells on routine trephine bone marrow biopsies. *Mod. Pathol.* **12**, 1101–1106.
- Fagioli, C., and Sitia, R. (2001). Glycoprotein quality control in the endoplasmic reticulum. Mannose trimming by endoplasmic reticulum mannosidase I times the proteasomal degradation of unassembled immunoglobulin subunits. *J. Biol. Chem.* **276**, 12885–12892.
- Frey, J.R., Fountoulakis, M., and Lefkowitz, I. (2000). Proteome analysis of activated murine B-lymphocytes. *Electrophoresis* **21**, 3730–3739.
- Grunenfelder, B., Rummel, G., Vohradsky, J., Roder, D., Langen, H., and Jenal, U. (2001). Proteomic analysis of the bacterial cell cycle. *Proc. Natl. Acad. Sci. USA* **98**, 4681–4686.
- Gygi, S.P., Corthals, G.L., Zhang, Y., Rochon, Y., and Aebersold, R. (2000). Evaluation of two-dimensional gel electrophoresis-based proteome analysis technology. *Proc. Natl. Acad. Sci. USA* **97**, 9390–9395.
- Haas, I.G., and Wabl, M. (1983). Immunoglobulin heavy chain binding protein. *Nature* **306**, 387–389.
- Hwang, C., Sinskey, A.J., and Lodish, H.F. (1992). Oxidized redox state of glutathione in the endoplasmic reticulum. *Science* **257**, 1496–1502.
- Ingolia, T.D., and Craig, E.A. (1982). Drosophila gene related to the major heat shock-induced gene is transcribed at normal temperatures and not induced by heat shock. *Proc. Natl. Acad. Sci. USA* **79**, 525–529.
- Kettman, J., and Lefkowitz, I. (1984). Changes in the protein pattern of murine B cells after mitogenic stimulation. *Eur. J. Immunol.* **14**, 778–781.
- Kokame, K., Kato, H., and Miyata, T. (2001). Identification of ERSE-II, a new cis-acting element responsible for the ATF6-dependent mammalian unfolded protein response. *J. Biol. Chem.* **276**, 9199–9205.
- Lee, A.S. (2001). The glucose-regulated proteins: stress induction and clinical applications. *Trends Biochem. Sci.* **26**, 504–510.
- Lee, K., Tirasophon, W., Shen, X., Michalak, M., Prywes, R., Okada, T., Yoshida, H., Mori, K., and Kaufman, R.J. (2002). IRE1-mediated unconventional mRNA splicing and S2P-mediated ATF6 cleavage merge to regulate XBP1 in signaling the unfolded protein response. *Genes Dev.* **16**, 452–466.
- Lin, H.Y., Masso-Welch, P., Di, Y.P., Cai, J.W., Shen, J.W., and Subjeck, J.R. (1993). The 170-kDa glucose-regulated stress protein is an endoplasmic reticulum protein that binds immunoglobulin. *Mol. Biol. Cell* **4**, 1109–1119.
- Lucero, H.A., Lebeche, D., and Kammer, B. (1998). ERcalcistorin/protein-disulfide isomerase acts as a calcium storage protein in the endoplasmic reticulum of a living cell. Comparison with calreticulin and calsequestrin. *J. Biol. Chem.* **273**, 9857–9863.
- Ma, Y., and Hendershot, L.M. (2001). The unfolding tale of the unfolded protein response. *Cell* **107**, 827–830.
- Mann, M., and Wilm, M. (1994). Error-tolerant identification of peptides in sequence databases by peptide sequence tags. *Anal. Chem.* **66**, 4390–4399.
- Melnick, J., Dul, J.L., and Argon, Y. (1994). Sequential interaction of the chaperones BiP and GRP94 with immunoglobulin chains in the endoplasmic reticulum. *Nature* **370**, 373–375.
- Ono, S.J., Liou, H.C., Davidon, R., Strominger, J.L., and Glimcher, L.H. (1991). Human X-box-binding protein 1 is required for the transcription of a subset of human class II major histocompatibility genes and forms a heterodimer with c-fos. *Proc. Natl. Acad. Sci. USA* **88**, 4309–4312.
- Patil, C., and Walter, P. (2001). Intracellular signaling from the endoplasmic reticulum to the nucleus: the unfolded protein response in yeast and mammals. *Curr. Opin. Cell Biol.* **13**, 349–355.
- Piskurich, J.F., Lin, K.I., Lin, Y., Wang, Y., Ting, J.P., and Calame, K. (2000). BLIMP-1 mediates extinction of major histocompatibility class II transactivator expression in plasma cells. *Nat. Immunol.* **1**, 526–532.
- Reddy, P.S., and Corley, R.B. (1999). The contribution of ER quality control to the biologic functions of secretory IgM. *Immunol. Today* **20**, 582–588.
- Reddy, P., Sparvoli, A., Fagioli, C., Fassina, G., and Sitia, R. (1996). Formation of reversible disulfide bonds with the protein matrix of the endoplasmic reticulum correlates with the retention of unassembled Ig light chains. *EMBO J.* **15**, 2077–2085.
- Reimold, A.M., Etkin, A., Clauss, I., Perkins, A., Friend, D.S., Zhang, J., Horton, H.F., Scott, A., Orkin, S.H., Byrne, M.C., et al. (2000). An essential role in liver development for transcription factor XBP-1. *Genes Dev.* **14**, 152–157.
- Reimold, A.M., Iwakoshi, N.N., Manis, J., Vallabhajosyula, P., Szomlanyi-Tsuda, E., Gravalles, E.M., Friend, D., Grusby, M.J., Alt, F., and Glimcher, L.H. (2001). Plasma cell differentiation requires the transcription factor XBP-1. *Nature* **412**, 300–307.
- Roy, B., and Lee, A.S. (1999). The mammalian endoplasmic reticulum stress response element consists of an evolutionarily conserved tripartite structure and interacts with a novel stress-inducible complex. *Nucleic Acids Res.* **27**, 1437–1443.
- Sealy, L., Mota, F., Rayment, N., Tatnell, P., Kay, J., and Chain, B. (1996). Regulation of cathepsin E expression during human B cell differentiation in vitro. *Eur. J. Immunol.* **26**, 1838–1843.
- Shachar, I., Amitay, R., Rabinovich, E., Haimovich, J., and Bar-Nun, S. (1992). Polymerization of secretory IgM in B lymphocytes is prevented by a prior targeting to a degradation pathway. *J. Biol. Chem.* **267**, 24241–24247.
- Shaffer, A.L., Lin, K.I., Kuo, T.C., Yu, X., Hurt, E.M., Rosenwald, A., Giltnane, J.M., Yang, L., Zhao, H., Calame, K., and Staudt, L.M. (2002). Blimp-1 orchestrates plasma cell differentiation by extinguishing the mature B cell gene expression program. *Immunity* **17**, 51–62.
- Shen, X., Ellis, R.E., Lee, K., Liu, C.Y., Yang, K., Solomon, A., Yoshida, H., Morimoto, R., Kumit, D.M., Mori, K., and Kaufman, R.J. (2001). Complementary signaling pathways regulate the unfolded protein response and are required for *C. elegans* development. *Cell* **107**, 893–903.
- Shevchenko, A., Sunyaev, S., Loboda, A., Bork, P., Ens, W., and Standing, K.G. (2001). Charting the proteomes of organisms with unsequenced genomes by MALDI-quadrupole time-of-flight mass spectrometry and BLAST homology searching. *Anal. Chem.* **73**, 1917–1926.
- Silacci, P., Mottet, A., Steimle, V., Reith, W., and Mach, B. (1994). Developmental extinction of major histocompatibility complex class

I $\kappa$  gene expression in plasmocytes is mediated by silencing of the transactivator gene CIITA. *J. Exp. Med.* **180**, 1329–1336.

Sitia, R., Rubartelli, A., Deambrosio, S., Pozzi, D., and Hammerling, U. (1985). Differentiation in the murine B cell lymphoma I.29: inductive capacities of lipopolysaccharide and *Mycoplasma fermentans* products. *Eur. J. Immunol.* **15**, 570–575.

Sitia, R., Neuberger, M.S., and Milstein, C. (1987). Regulation of membrane IgM expression in secretory B cells: translational and post-translational events. *EMBO J.* **6**, 3969–3977.

Sitia, R., Neuberger, M., Alberini, C., Bet, P., Fra, A., Valetti, C., Williams, G., and Milstein, C. (1990). Developmental regulation of IgM secretion: the role of the carboxy-terminal cysteine. *Cell* **60**, 781–790.

Stavnezer, J., Sirlin, S., and Abbott, J. (1985). Induction of immunoglobulin isotype switching in cultured I.29 B lymphoma cells. Characterization of the accompanying rearrangements of heavy chain genes. *J. Exp. Med.* **161**, 577–601.

Trombetta, E.S., and Helenius, A. (1998). Lectins as chaperones in glycoprotein folding. *Curr. Opin. Struct. Biol.* **8**, 587–592.

Tu, B.P., and Weissman, J.S. (2002). The FAD- and O(2)-dependent reaction cycle of Ero1-mediated oxidative protein folding in the endoplasmic reticulum. *Mol. Cell* **10**, 983–994.

Turner, C.A., Jr., Mack, D.H., and Davis, M.M. (1994). Blimp-1, a novel zinc finger-containing protein that can drive the maturation of B lymphocytes into immunoglobulin-secreting cells. *Cell* **77**, 297–306.

Wang, Y., Shen, J., Arenzana, N., Tirasophon, W., Kaufman, R.J., and Prywes, R. (2000). Activation of ATF6 and an ATF6 DNA binding site by the endoplasmic reticulum stress response. *J. Biol. Chem.* **275**, 27013–27020.

Wiest, D.L., Burkhardt, J.K., Hester, S., Hortsch, M., Meyer, D.I., and Argon, Y. (1990). Membrane biogenesis during B cell differentiation: most endoplasmic reticulum proteins are expressed coordinately. *J. Cell Biol.* **110**, 1501–1511.

Wilm, M., Shevchenko, A., Houthaeve, T., Breit, S., Schweigerer, L., Fotsis, T., and Mann, M. (1996). Femtomole sequencing of proteins from polyacrylamide gels by nano-electrospray mass spectrometry. *Nature* **379**, 466–469.

Yoshida, H., Haze, K., Yanagi, H., Yura, T., and Mori, K. (1998). Identification of the cis-acting endoplasmic reticulum stress response element responsible for transcriptional induction of mammalian glucose-regulated proteins. Involvement of basic leucine zipper transcription factors. *J. Biol. Chem.* **273**, 33741–33749.

Yoshida, H., Matsui, T., Yamamoto, A., Okada, T., and Mori, K. (2001). XBP1 mRNA is induced by ATF6 and spliced by IRE1 in response to ER stress to produce a highly active transcription factor. *Cell* **107**, 881–891.

Zhang, W., and Chait, B.T. (2000). ProFound: an expert system for protein identification using mass spectrometric peptide mapping information. *Anal. Chem.* **72**, 2482–2489.